Ind. J. Pharm. Edu. Res., 2025; 59(2s):s443-s453.
https://www.ijper.org

Original Article

Optimizing Loratadine Delivery: Development of Niosomal Transdermal Patches

Charan Sailaja[1], Pradeep Kumar Bhupalam[2,*]

[1]Department of Pharmaceutical Sciences, JNTUA, Ananthapuramu, Andhra Pradesh, INDIA.
[2]Department of Pharmacology, Raghavendra Institute of Pharmaceutical Education and Research (RIPER)-(Autonomous, K. R. Palli Cross, Ananthapuramu, Affiliated to JNTUA), Ananthapuramu, Andhra Pradesh, INDIA.

ABSTRACT

Objectives: To improve and optimize loratadine-loaded niosomal transdermal patches with a Box-Behnken Design to enhance drug delivery and evaluate their potential as an effective alternative to oral administration for allergy treatment. **Materials and Methods:** Span 40 and Span 80. A Box-Behnken Design (BBD) implemented in Design Expert software was employed to assess the impact of these surfactants on vesicle size, zeta potential and drug entrapment efficiency. Additional physicochemical properties of the niosomes were characterized. The optimized formulation was subsequently incorporated into transdermal patches via solvent casting. These patches were evaluated for flexibility, uniformity and weight and their drug release was compared to a conventional transdermal patch. **Results:** The niosomal formulation LN-14, optimized with Span 20, Span 40 and Span 80, exhibited superior characteristics, including the smallest vesicle size (195±0.55 nm), highest zeta potential (-54.25±0.08 mV) and maximum entrapment efficiency (91.14±2.95%), leading to its selection for transdermal patch development. The resulting patches were consistent in thickness, weight and flexibility, with strong tensile properties. The LRD-loaded niosomal patches demonstrated a sustained drug release profile, with over 40% permeation by the 4th hr and sustained release over 42 hr, showing potential for effective transdermal delivery. **Conclusion:** The study revealed that niosomal patches demonstrated effective transdermal delivery of loratadine, offering a promising alternative to oral administration with the potential to reduce gastrointestinal adverse effects. These findings suggest that niosomal patches may be a viable approach for the topical treatment of allergies.

Keywords: Box-Behnken design, Entrapment efficiency, Loratadine-loaded niosomes, Niosomal patches, Transdermal delivery.

Correspondence:
Dr. Pradeep Kumar Bhupalam
Department of Pharmacology, Raghavendra Institute of Pharmaceutical Education and Research (RIPER)-(Autonomous, K. R. Palli Cross, Ananthapuramu, Affiliated to JNTUA), Ananthapuramu-515001, Andhra Pradesh, INDIA.
Email: bhupalampradeep@gmail.com

Received: 10-08-2024;
Revised: 17-10-2024;
Accepted: 15-01-2025.

INTRODUCTION

Transdermal patches offer a superior drug delivery method compared to traditional oral or injectable forms. They bypass the digestive system and deliver medication directly through the skin, they ensure a consistent and sustained discharge of the drug into the bloodstream.[1] This leads to improved drug bioavailability, meaning a higher proportion of the medication reaches the intended target site. As a result, patients experience more effective and sustained therapeutic benefits.[2] Additionally, the avoidance of the gut significantly reduces the likelihood of common side effects associated with oral medications. The non-invasive nature of transdermal patches enhances patient comfort and compliance, particularly for chronic conditions requiring long-term treatment. While not suitable for all drugs due to factors such as molecular weight and skin permeability, transdermal patches represent a promising and evolving technology with the potential to revolutionize drug delivery.[3]

Loratadine (LRD) is a non-sedating antihistamine widely used to alleviate allergy symptoms such as sneezing, runny nose, itchy eyes and hives.[4] It works by blocking the effects of histamine, a substance discharged by the body during allergic reactions. Unlike older-generation antihistamines, LRD does not cause drowsiness, making it an ideal choice for individuals who need to stay alert while managing their allergy symptoms.[5]

Niosomes are microscopic, spherical structures composed primarily of non-ionic surfactants. These surfactants are molecules with both water-loving (hydrophilic) and oil-loving (hydrophobic) parts, allowing them to form a bilayer structure similar to cell membranes.[6] This bilayer creates a protective shell around an internal aqueous compartment where drugs can be encapsulated.[7] They can accommodate a wide range of drugs, from water-soluble (hydrophilic) to fat-soluble (hydrophobic) compounds.[8] This flexibility makes them suitable for delivering

DOI: 10.5530/ijper.20250564

various medications. Once a drug is encapsulated within the niosome, it is protected from degradation and can be discharged in a sustained manner.[9] This sustained discharge can prolong the drug's effect, reduce dosing frequency and minimize side effects. Additionally, niosomes can be designed to target specific organs or tissues, enhancing drug delivery efficiency.[10] Compared to liposomes (another type of vesicle), niosomes offer several advantages. They are generally more stable, less expensive to produce and better tolerated by the body.[11] These characteristics make niosomes a promising platform for delivering a variety of therapeutic agents, including vaccines, anticancer drugs and treatments for various diseases.

By encapsulating antihistamines like LRD within niosomes, drug delivery to the skin the primary site of allergic reactions can be enhanced.[12] Niosomes can improve drug solubility and sustained discharge and potentially target specific skin layers. Combined with the sustained release properties of transdermal patches, this method can provide prolonged relief from allergy symptoms, reducing the need for frequent dosing. Additionally, by avoiding the oral route, niosomal patches can minimize systemic side effects commonly associated with oral antihistamines, offering a more targeted and effective treatment option.[12]

The empirical approach is time-consuming, resource-intensive and often results in suboptimal formulations.[13] QbD, in contrast, employs a systematic approach to understanding the Critical Quality Attributes (CQAs) of a product and identifies the Critical Process Parameters (CPPs) that influence them. By establishing a design space, QbD ensures product quality, consistency and efficacy from the outset.[14-16] This proactive approach reduces the risk of formulation failures, accelerates development timelines and ultimately leads to superior product performance.

This study aimed to optimize loratadine-loaded niosomal transdermal patches using a Box-Behnken Design. The influence of Span 40 and Span 80 on vesicle size, zeta potential and drug entrapment efficiency was evaluated. Optimized niosomes were incorporated into transdermal patches and their permeation was compared to a conventional transdermal patch.

MATERIALS AND METHODS

Materials

Loratadine was procured from Cipla Ltd., Bengaluru. Cholesterol, Span 20, Span 40, Span 80, dichloromethane and dicetyl phosphate, were obtained from Merck. Double-distilled water and buffers at pH 6 and 7.4 were prepared in-house.

Fabrication of the LRD niosomes

Loratadine-Loaded Niosomes (LN) was made using the ether injection method. Cholesterol (50 mg) was dissolved in dichloromethane, while a mixture of Span 20, Span 40 and Span 80 was dissolved in diethyl ether. LRD (100 mg) was added to methanol and combined with the surfactant solution. Dicetyl Phosphate (DCP) was incorporated as needed. The resulting mixture was slowly injected into phosphate buffer saline (PBS, pH 7.4) using a syringe pump at a rate of 1 mL/min while stirring continuously at 60±5°C. The temperature differential induced solvent evaporation, resulting in the formation of niosomes (Table 1).[17-19]

Refinement of niosomes

To distinguish the free LRD from the niosomal formulation, gel filtration chromatography was employed. Initially, a 0.2 mL aliquot of the prepared niosomal formulation was carefully applied to a Sephadex G50 minicolumn, a medium commonly used for separating molecules based on size. The column was then subjected to centrifugation at 6000 rpm for 1 hr, with PBS of pH 7.4 serving as the eluent. This process allowed the niosomes, which are larger, to be eluted separately from the smaller, unentrapped drug molecules. As the niosomes passed through the column, they were effectively separated from any free drug that was not encapsulated. After the centrifugation process, the purified niosomal formulation was collected and carefully transferred to amber glass vials. These vials, known for protecting light-sensitive substances, were filled with PBS (pH 7.4) to maintain the stability of the niosomes. The purified niosomal formulation was then stored under appropriate conditions until further use or analysis. This purification step is crucial to ensure that subsequent studies on the niosomal formulation accurately reflect the behavior of the encapsulated drug without interference from the free, unentrapped drug.[20,21]

PS, PDI and ZP

The PS, PDI and ZP of the niosomal suspensions were assessed using Photon Correlation Spectroscopy (PCS) with a Zetasizer (Nano ZS90 instrument). Before measurement, the samples were diluted appropriately. Vesicle size and PDI were measured at a scattering angle of 90° and a temperature of 25°C. The electrophoretic mobility of the particles was converted to ZP using the Smoluchowski equation under the same conditions.[22,23]

EE of the niosomes

The % EE of LRD was resolute indirectly by comparing the total amount of LRD in the formulation to the amount lasting in the aqueous phase after centrifuging the niosomal suspension at 15,000 rpm for 1 hr at 4°C. The supernatant was then analyzed spectrophotometrically at 243.5 nm to quantify the free LRD. The % EE was calculated by finding the difference between the total LRD and the free LRD (e.q. 1).[24,25]

$$EE = \frac{\text{Entrapped LRD}}{\text{Total LRD added}} \times 100 \text{--- (1)}$$

Optimization

Niosomes were formulated using different levels of Span 20, Span 40 and Span 80 (25, 37.5 and 50 mg) under various hydration conditions. The optimal niosomal formulation was calculated based on PS, ZP and SI. Throughout the experiments, a constant aqueous phase volume of 10 mL was maintained to ensure consistency in the formulation process.[26,27]

In vitro permeation

In vitro, drug permeation was assessed using the dialysis bag. Dialysis bags were pre-treated by soaking in PBS for 24 hr. A diluted niosomal suspension (in PBS) was then enclosed in a dialysis bag and submerged in 20 mL of 20% isopropanol-PBS. The system was incubated at 37°C with continuous agitation at 100 rpm for 24 hr. To maintain sink conditions, samples were collected at fixed times and replaced with fresh medium. The drug concentration in the collected samples was measured using UV spectrophotometry at 243.5 nm.[28,29]

The niosomal formulation (LN-14) demonstrated superior characteristics, including smaller vesicle size, higher zeta potential and improved entrapment efficiency compared to other formulations. These enhancements were attributed to its optimized ratios of Span 20, Span 40 and Span 80. Based on these promising results, LN-14 was selected for further development as a transdermal patch.

Preparation of LRD-loaded niosomal patch

Niosomal patches were fabricated using 5% w/v of Propylene Glycol (PG) as a plasticizer and aqueous solutions of HPMC and Na-CMC (1:1). The components were thoroughly mixed using a magnetic stirrer, followed by sonication to remove air bubbles. The resulting mixture was spread on glycerine-coated Petri dishes and dried in a 40°C oven. The dried film was backed with an EVA fabric and sealed with a PVP liner. The completed LN-14 patches were stored in a desiccator.[30-32]

Assessing the patches

Physical appeal

The physical characteristics of the transdermal patches were assessed through visual inspection and measurement. The patches were examined for their overall appearance, including their color (uniformity and intensity), transparency (or opacity), flexibility (ability to bend without cracking) and surface smoothness.[33]

To quantify the thickness of the patches, a precise measuring instrument called a micrometer was used. For each batch of patches, three individual patches were randomly selected. The thickness of each patch was measured at multiple points and these measurements were averaged to find the mean thickness of the batch. This approach helps to ensure that the reported thickness is representative of the overall patch consistency.

Uniformity in weight

To evaluate the weight consistency of the transdermal patches, a quality control measure was implemented. For each unique formulation of the patch, a total of three patches were selected randomly from the batch. This random selection helped to ensure that the sample was representative of the entire production. Each of the three selected patches was weighed individually using a precise weighing scale. The obtained weights were then averaged to calculate the mean weight for that specific formulation batch. This process was repeated for all formulations under investigation. By comparing the average weights of different batches, it was possible to assess the weight uniformity and reproducibility of the patch manufacturing process. This method helps to identify any significant variations in patch weight, which could potentially affect drug delivery and product performance.[34]

Folding Endurance

It is a measure of a material's flexibility and resistance to cracking or breaking when subjected to repeat folding at the same location. In this specific experiment, a film was subjected to continuous folding at a single point until it ruptured. The number of folds the film could withstand before breaking was recorded. A higher

Table 1: Various formulations of LN.

Independent variables	Levels		
	Low	Medium	High
X_1=Span 20 (mg)	25	37.5	50
X_2=Span 40 (mg)	25	37.5	50
X_3=Span 80 (mg)	25	37.5	50
Distorted values	-1	0	+1
Responses observed	Conditions		
Y_1=Vesicle size (nm)	Minimize		
Y_2=Entrapment efficiency (%)	Maximize		
Y_3=Zeta potential (mV)	Maximize		

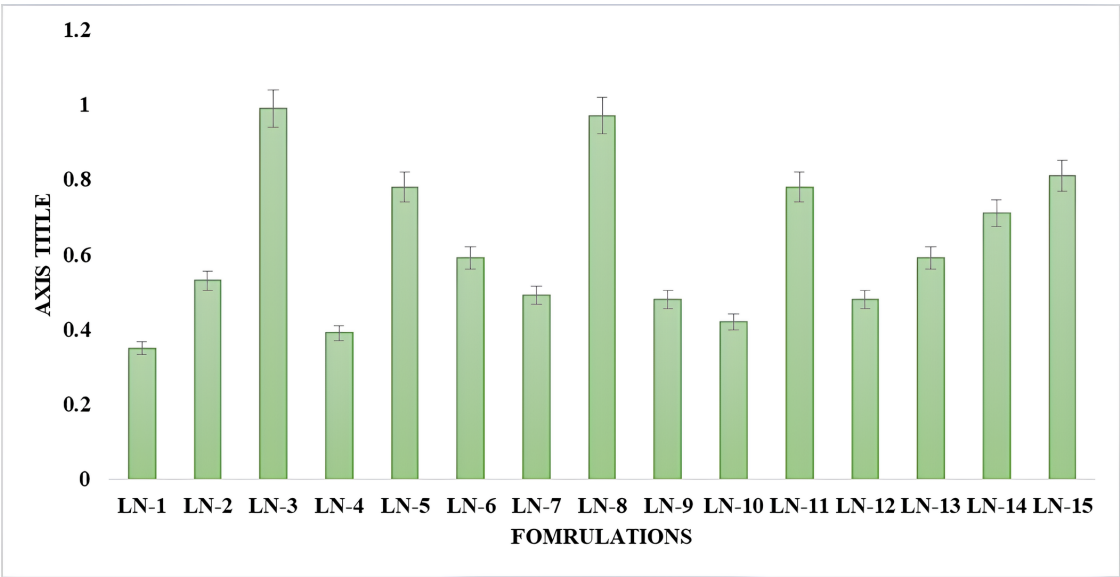

Figure 1: PDI of the niosomal formulations.

Table 2: Physicochemical assets of LN.

Formulation	VS (μM)	ZP (mV)	% LRD content	EE (%)	DR (%)
LN-1	312±2.34	45.89±2.15	89.58±1.25	85.60±0.52	89.22±2.94
LN-2	334±1.26	40.00±1.16	95.62±2.36	83.60±1.31	93.25±4.15
LN-3	200±3.25	50.00±3.25	89.88±2.55	90.60±1.98	95.23±0.65
LN-4	401±4.18	38.62±0.11	92.34±1.85	79.69±0.25	94.35±3.84
LN-5	215±7.25	52.62±1.25	93.16±1.65	88.27±0.57	93.66±2.65
LN-6	384±6.26	39.65±1.12	90.15±2.84	80.25±0.91	96.00±2.36
LN-7	271±2.85	46.96±2.02	88.27±1.95	86.00±1.04	92.31±1.25
LN-8	324±4.15	44.25±1.05	89.97±2.65	84.50±0.06	93.15±5.66
LN-9	375±3.26	40.25±1.08	91.28±4.24	81.60±0.15	94.28±1.03
LN-10	224±2.08	49.88±2.64	90.28±6.32	87.00±1.61	91.23±2.74
LN-11	255±3.15	48.96±2.54	92.48±2.84	86.32±2.54	93.98±3.03
LN-12	345±2.68	41.25±1.15	93.87±3.99	82.60±3.45	92.54±1.84
LN-13	206±1.98	53.96±3.78	97.05±1.47	88.90±2.15	92.07±2.61
LN-14	195±1.25	53.00±1.78	93.88±5.65	91.14±2.95	94.84±5.02
LN-15	201±2.36	54.25±0.08	92.36±4.44	89.60±1.51	90.51±2.47

Values in mean±SD; *n*=3.

folding endurance indicates a more flexible and durable film. This test is crucial for evaluating the mechanical properties of materials used in applications that require frequent bending or folding, such as packaging materials, medical films and textile fabrics.[35]

Tensile strength

A rectangular film strip with dimensions of 40 mM by 15 mM was used for the tensile strength test. To ensure proper handling and alignment during the test, one end of the film was secured to an adhesive tape mounted on a film holder. This provided a stable base for the film. A simple yet effective setup was employed. A small pin was positioned between the adhesive tapes at the free end of the film to maintain its straight orientation during the stretching process. A tiny hole was created in the adhesive tape near the pin to accommodate a hook. A thread was attached to this hook and passed over a pulley. At the other end of the thread, a small pin was used to hold weights that would apply tension to the film. A pointer connected to the thread moved across a graph paper scale, indicating the displacement caused by the applied force. The tensile strength test was conducted by gradually increasing the load on the film. This was achieved by incrementally adding weights to the pan attached to the thread. As the weight increased, the tensile force exerted on the film grew,

causing it to elongate. The point at which the film ruptured was observed and the corresponding weight on the pan represented the breaking force. The displacement of the pointer on the graph paper provided a qualitative measure of the film's elongation before failure. However, this setup did not allow for precise calculation of stress and strain, which are typically required for a comprehensive analysis of tensile properties. While this method provides a basic understanding of the film's tensile strength, modern tensile testing machines offer more accurate and detailed measurements of stress, strain and other mechanical properties. This experimental setup provides a fundamental approach to evaluating the tensile strength of a film, but it is essential to consider its limitations when interpreting the results.[36,37]

Drug content analysis

To assess drug release characteristics, standardized one-centimeter square sections were excised from each transdermal patch and submerged in 100 mL of PBS, a physiological mimic. Continuous agitation was induced using a magnetic bead to optimize drug extraction. Subsequent filtration through Whatman filter paper removed particulates, yielding a drug-laden filtrate. Spectrophotometric analysis at 243.5 nm quantified the released drug concentration against a drug-free control. To ensure data reliability, the experimental protocol was rigorously replicated, providing a robust evaluation of the transdermal patch's drug delivery profile.[38,39]

In vitro diffusion study

Franz diffusion cells, equipped with 22 mL receptor compartments filled with pH 7.4 phosphate buffer, were employed for *in vitro* diffusion studies. Transdermal patches, affixed to cellophane membranes, were mounted on the donor compartment, ensuring direct contact with the receptor fluid. The entire assembly was maintained at 32±0.5°C using a water bath. To monitor drug permeation, aliquots were extracted from the receptor compartment at predetermined intervals and replenished with fresh buffer, facilitating continuous diffusion while maintaining sink conditions. The collected samples underwent spectrophotometric analysis to quantify drug concentration.[40]

RESULTS

Physicochemical assets

The prepared niosomal formulations exhibited uniform VS ranging from 195±0.55 nm (LN-14) to 401±1.41 nm (LN-4). ZP values varied from -38.62±0.11 mV (LN-4) to -54.25±0.08 mV (LN-15), indicating good stability of the niosomal systems. The EE% of LRD within the niosomes ranged from 79.69±0.25% (LN-4) to 91.14±2.95% (LN-14), with LN-14 demonstrating the highest entrapment. LRD loading was observed to be between 89.88±2.55% (LN-3) and 97.05±1.47% (LN-13). The LRD discharge profile showed the lowest discharge for LN-1 (89.22±2.9%) and the highest for LN-6 (96.00±2.36%) (Table 2).

PDI

The Polydispersity Index (PDI) of the LN varied significantly, ranging from 0.38±0.01 (LN-1) to 0.98±0.02 (LN-3). A lower PDI value of 0.38±0.01 in LN-1 indicates a more uniform VS distribution, suggesting that the niosomes in this formulation are more consistent in size and shape. This uniformity is often associated with better stability and predictable drug discharge profiles. On the other hand, a higher PDI value of 0.98±0.02 in LN-3 indicates a broader VS distribution, implying greater variability in the size of the niosomes, which could affect the stability and consistency of drug discharge. These results highlight the importance of optimizing formulation constraints to get a desirable PDI, which is crucial for certifying the efficacy and reliability of the niosomal drug delivery system (Figure 1).

Optimization of the LN

The analysis of the final equations resulting using coded factors revealed critical visions into the dealings between the IVs namely, the concentrations of Span 20, Span 40 and Span 80 with their corresponding responses, which include VS, ZP and %EE. These equations proved to be effective predictive tools, allowing for the estimation of response values based on specific levels of these factors. Each equation highlighted how individual factors (X_1 for Span 20, X_2 for Span 40 and X_3 for Span 80) and their interactions (X_1X_2, X_1X_3 and X_2X_3) impacted the responses. The results indicated that positive coefficients in these equations suggested that increasing the levels of the respective factors would enhance the response. Conversely, negative coefficients indicated a reduction in the response with an increase in the factor levels. For instance, in cases where the coefficient for Span 20 (X_1) was positive, an increase in Span 20 concentration led to an improvement in VS or % EE. On the other hand, a negative coefficient for Span 40 (X_2) suggested that a higher concentration of Span 40 might reduce the ZP and VS. The interaction terms (X_1X_2, X_1X_3 and X_2X_3) further illustrated how combinations of these surfactants prejudiced the formulation outcomes. These interactions were crucial in understanding the synergistic or antagonistic effects of the surfactants when used together, which significantly affected the final niosome characteristics. The equations can be expressed as follows:

$$PS=+200.67+55.63A-13.25B-0.38C+44.75AB-29AC+60.3BC+54.92A^2+56.17B^2+42.92C^2$$

$$EE=+89.87-2.72A+0.2737B+0.294C-2.08AB+1.61AC-2.3BC-2.39A^2-2.75B^2-2.74C^2$$

$$ZP=+53.74-4.12A+0.5812B-0.123C-1.37AB+2.56AC-4.3BC-4.66A^2-5.45B^2-3.20C^2$$

Table 3: Statistical instant of the quadratic responses.

Response	Sequential *p*-value	Lack of Fit *p*-value	Adjusted R^2	Predicted R^2
PS	<0.0001	0.7772	0.9966	0.9910
% EE	0.0016	0.7602	0.9358	0.8268
ZP	<0.0001	0.7511	0.9912	0.9757

The fit statistics and ANOVA for the quadratic models of VS, ZP and % EE are summarized in Table 4.

Table 4: Fit statistics and ANOVA for the quadratic model.

Parameter	PS	% EE	ZP
Std. Dev.	4.38	0.9072	0.5323
Mean	282.80	85.66	46.64
C.V. %	1.55	1.06	1.14
Adeq Precision	56.1357	13.1703	34.559
Lack of fit F-value	0.3874	0.4191	0.4365
Lack of fit *p*-value	0.7772	0.7602	0.7511
Model F-value	450.50	23.69	175.31
Model *p*-value	<0.0001	0.0014	<0.0001

The statistical summary of the quadratic responses for VS, ZP and %EE is presented in Table 3. The sequential *p*-values for the quadratic models were highly significant for all three responses: <0.0001 for VS and ZP and 0.0016 for EE. These low *p*-values indicate that the quadratic models are statistically significant and effectively capture the relationship between the Independent Variables (IVs) and the responses. The Lack of Fit *p*-values, which assess whether the model adequately fits the data, were 0.7772 for vesicle 0.7602 for EE and 0.7511 for ZP. These high *p*-values suggest that there was no significant lack of fit for the models, indicating that the quadratic models were appropriate for describing the data. The Adjusted R^2 values, which reflect the proportion of variance explained by the models while accounting for the number of predictors, were 0.9966 for VS, 0.9358 for EE and 0.9912 for ZP. These high Adjusted R^2 values indicate that the models provide an excellent fit to the experimental data and account for a substantial amount of variability in the responses. The Predicted R^2 values, which assess the model's ability to predict new data, were 0.9910 for VS, 0.8268 for EE and 0.9757 for ZP. These values are also high, indicating that the models have strong predictive capabilities and can be reliably used to forecast response values based on new experimental conditions (Table 3).

Contour plots illustrate the relationships between the levels of Span 20, Span 40 and Span 80 and the responses of VS, Zp and %EE. These plots provide a two-dimensional view of how changes in these factors influence the responses. The contour lines reveal regions where the response values remain constant, showing how varying one factor while holding others constant affects the response. The 3D plots offer a three-dimensional perspective on the interactions between Span 20, Span 40 and Span 80 levels and their impact on the responses. These plots help visualize how changes in the levels of these factors influence the responses more comprehensively. By adjusting the levels of Span 20, Span 40 and Span 80, the 3D plots highlight the combined effects of these factors on the response variables, showing areas where optimal responses can be achieved. Cubic plots display the relationships between the IVs (Span 20, Span 40 and Span 80) and the responses through a three-dimensional surface. These plots provide insight into the non-linear interactions among the factors and their effects on VS, ZP and % EE. The cubic plots illustrate how combinations of different levels of the factors affect the responses, helping to identify optimal conditions for achieving desired results (Figure 2).

Physicochemical assets of the prepared patches

The prepared transdermal patches (with LN-14) exhibited favorable physicochemical properties. The visual inspection revealed that the patches had an appealing appearance, characterized by uniform color, clarity and a smooth surface texture. Measurements confirmed uniform thickness (49.77±2.19 mM) and weight (1.42±0.08 g) across the patches, indicating consistent formulation and manufacturing processes. The patches demonstrated high flexibility, as evidenced by their substantial folding endurance (128±3). Additionally, the tensile strength tests showed that the patches possessed adequate strength (89.96±1.66 g/cm^2), capable of resisting tearing and stretching under stress.

In vitro drug permeated

The LNP has undergone a 42 hr *in vitro* drug permeation study to check the permeation profile of LRD. The LNP exhibited a controlled but gradually increasing permeation of LRD, with > 40% permeation observed by the 4th hr at pH 6. The permeation

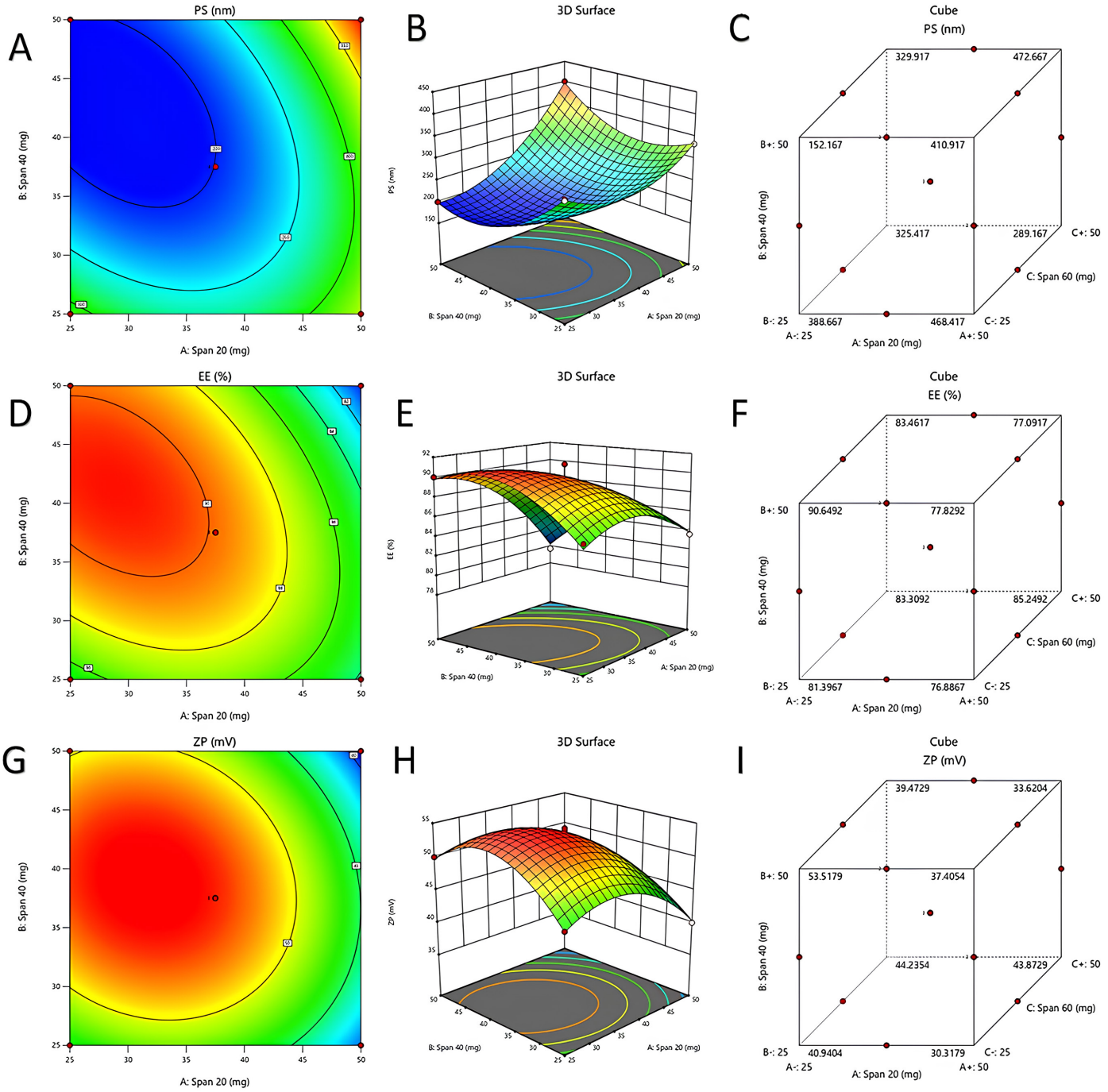

Figure 2: Contour plots (A, D and G); 3D plots (B, E and H); and cubic models (C, F and I) representing the impact of inputs on the responses.

study continued over 42 hr, during which all LNP formulations demonstrated continuous and sustained drug permeation. The release kinetics of LRD from the optimized LNP were assessed using a linear regression equation, yielding the equation Y = 1.5344x+33.078 with an r^2 value of 0.7173 at pH 6. This indicates a consistent and sustained discharge pattern over the 42 hr study period. In contrast, the normal patch without niosomal encapsulation exhibited a discharge profile represented by the equation Y = 0.6496x+14.29 with an r^2 value of 0.7406 (Figure 3).

DISCUSSION

The obtained results demonstrate the successful formation of niosomal formulations with varying VS and ZP. The negative ZP values suggest good stability of the niosomes, reducing the likelihood of aggregation. The high EE achieved for most formulations indicates the suitability of the niosomal carrier for LRD delivery. The variation in drug loading and discharge profiles among the different formulations highlights the influence of formulation parameters on the overall performance of the niosomal system. Further optimization of these parameters could

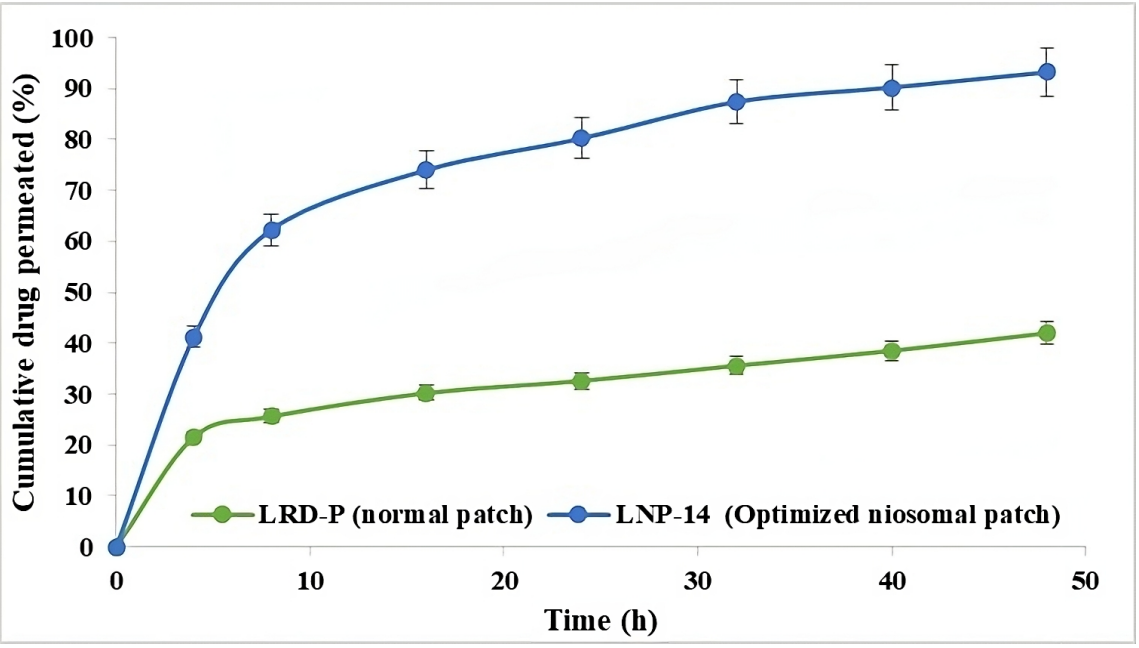

Figure 3: *In vitro* permeation of LNP vs. normal patch.

lead to the development of niosomal patches with tailored LRD discharge characteristics. The observed differences in VS, EE and ZP could be attributed to factors such as surfactant composition, cholesterol content and hydration conditions employed during the niosome preparation process. A deeper understanding of these relationships would require further investigations.[41]

The PDI values obtained for the niosomal formulations indicate varying degrees of PDI. Lower PDI values, such as that observed for LN-1, suggest a more uniform PDI, which is generally desirable for drug delivery systems. Conversely, higher PDI values, as seen in LN-3, imply a broader PDI. The PDI can be influenced by factors such as surfactant composition, lipid content and preparation method. Optimizing these parameters can lead to the development of niosomal formulations with improved homogeneity and potentially enhanced drug delivery performance.[42]

The derived equations offer a robust framework for understanding and optimizing the formulation of niosomes by illustrating the complex interactions between the surfactants and their impact on key parameters like VS, ZP and % EE. The positive coefficients observed in the equations emphasize the potential for certain surfactants, such as Span 20, to enhance formulation characteristics when used at higher concentrations. This is particularly important for optimizing VS and EE%, which are critical factors in the efficacy of niosomal drug delivery systems. Conversely, the negative coefficients provide cautionary insights, indicating that certain concentrations or combinations of surfactants might lead to less desirable outcomes, such as decreased stability or reduced drug loading capacity. For example, the negative impact of Span 40 at higher concentrations on ZP underscores the need to carefully balance surfactant levels to maintain optimal niosome stability. The interaction terms within the equations underscore the importance of understanding how different surfactants work together, as these interactions can have significant effects on the formulation. The synergistic effects identified through positive interaction coefficients suggest that certain combinations of surfactants can be used to achieve superior niosome characteristics. This knowledge enables researchers to fine-tune the formulation, enhancing the therapeutic potential of the niosomes by ensuring that the drug is delivered efficiently and effectively.[43]

The statistical analysis of the formulation parameters demonstrates that the models used to predict VS, ZP and %EE were robust and reliable. The low standard deviations and coefficient of variation percentages indicate that the measurements were consistent and repeatable across the experiments. The mean values for VS, % EE and ZP are within the expected ranges, suggesting that the niosomal formulations were well-optimized. The high adequate precision values further confirm the models' reliability in predicting the responses, highlighting the strong signal-to-noise ratios. The lack of significant lack of fit for all three parameters indicates that the models were well-suited for the data, with no evidence of systematic errors in the predictions. The highly significant model F-values and corresponding *p*-values underscore the strong relationship between the IVs and the responses. These results validate the use of the experimental design and optimization process employed in this study, demonstrating the effectiveness of the formulation strategies in achieving desirable VS, ZP and %EE for the niosomal formulations. This analysis not only supports the efficacy of the optimized formulations but also provides a solid foundation for future development and refinement of niosomal drug delivery systems.[44]

The statistical analysis of the quadratic responses highlights the robustness and accuracy of the models used for predicting VS, ZP and %EE. The significant sequential *p*-values for all responses confirm that the quadratic models are appropriate for describing the relationship between the IVs and the outcomes. The high Lack of Fit *p*-values suggests that the models fit the data well, with no evidence of systematic discrepancies. This supports the validity of the quadratic models and their effectiveness in capturing the underlying trends in the data. The Adjusted R^2 values indicate that the models provide a very good fit to the data, explaining a large proportion of the variability in the responses. This is particularly notable for VS and ZP, which have Adjusted R^2 values close to 1, signifying an almost perfect fit. The Predicted R^2 values, while slightly lower for EE, still demonstrate that the models have strong predictive capabilities. The consistency between the Adjusted and Predicted R^2 values further validates the models' reliability and their potential for guiding future experimental design and optimization.[45]

The fit statistics and ANOVA results confirm the robustness and validity of the quadratic models used to predict VS, ZP and % EE. The low SDs and C.V. percentages across all responses suggest that the experimental measurements are relatively consistent and precise. The Adequate Precision values indicate that the models have strong predictive capabilities and can navigate the design space effectively. The Lack of Fit F-values and *p*-values are high, demonstrating that the quadratic models do not exhibit a significant lack of fit and are therefore appropriate for describing the experimental data. This supports the reliability of the models in capturing the relationships between the formulation parameters and the responses. The very high Model F-values and low *p*-values signify that the quadratic models are statistically significant and capable of accurately representing the properties of the IVs on the responses. This indicates that the models are well-suited for optimizing the formulation parameters to achieve the desired VS, ZP and % EE.[46]

The contour plots, 3D plots and cubic plots collectively enhance our understanding of how varying levels of Span 20, Span 40 and Span 80 impact VS, ZP and % EE. The contour plots reveal specific regions where changes in Span 20, Span 40 and Span 80 lead to stable responses. This information is crucial for identifying ranges of factor levels that produce consistent vesicle sizes, high EE and desirable zeta potentials. By examining these plots, researchers can pinpoint optimal conditions and avoid configurations that may lead to suboptimal responses. The 3D plots provide a more nuanced view of the interactions between the factors. They show how simultaneous changes in Span 20, Span 40 and Span 80 affect the responses, highlighting regions where the responses improve or deteriorate. These plots are valuable for understanding the combined effects of multiple factors and for guiding the formulation of niosomes with desired properties. Cubic Plots: The cubic plots illustrate the non-linear dealings between the factors and responses. By showcasing the surface interactions, these plots help identify complex dependencies and interactions that may not be evident from linear models. The cubic plots are instrumental in exploring the full range of possible outcomes and in optimizing the formulation process to achieve the best results.[47]

The *in vitro* permeation study of LRD from the LNP demonstrated a superior and sustained permeation compared to the normal patch. The LNP achieved more than 40% drug permeation within the first 4 hr at pH 6, indicating an initial rapid diffusion followed by a controlled and sustained permeation over the subsequent hours. This gradual and consistent diffusion is advantageous for maintaining therapeutic drug levels over a lengthy time, potentially minimizing the frequency of dosing and refining patient obedience. The linear regression analysis further supports the controlled permeation behavior of the LNP, as reflected by the higher slope (1.5344) and intercept (33.078) in the LNP's diffusion equation compared to the normal patch. The r^2 value of 0.7173 for the LNP indicates a strong correlation between time and drug diffusion, suggesting that the LNP formulation is effective in providing a sustained permeation of LRD. In comparison, the normal patch's lower slope (0.6496) and intercept (14.29) indicate a less sustained permeation, which could lead to fluctuations in drug levels and potentially reduced efficacy. The slightly higher r^2 value of 0.7406 for the normal patch suggests a more predictable diffusion pattern, but the overall permeation rate is significantly lower than that of the LNP.[48]

CONCLUSION

The study successfully developed loratadine-loaded niosomal transdermal patches using a Box-Behnken Design, demonstrating their potential as an effective alternative to oral administration for allergy treatment. The results indicate that the niosomal formulations exhibit good stability, high entrapment efficiency and promising physicochemical properties, making them suitable candidates for drug delivery. The variations in drug loading and release profiles emphasize the importance of optimizing formulation parameters to achieve tailored drug release characteristics. The study's findings underscore the significant impact of surfactant composition, cholesterol content and preparation methods on niosomal performance. Furthermore, the statistical analysis validated the robustness and reliability of the models used to predict key parameters, such as vesicle size, zeta potential and entrapment efficiency. The *in vitro* permeation studies confirmed that the niosomal patches provide a superior and sustained release of loratadine compared to conventional patches, potentially enhancing therapeutic outcomes and patient compliance. Overall, this study lays a strong foundation for further development and clinical application of niosomal transdermal patches as a viable drug delivery system.

ACKNOWLEDGEMENT

The authors are thankful to the college management and the affiliated university for providing the facilities for performing the work.

CONFLICT OF INTEREST

The authors declare no conflict of interest.

ABBREVIATIONS

LRD: Loratadine; **BBD:** Box-Behnken Design; **PS:** Particle Size; **PDI:** Polydispersity Index; **ZP:** Zeta Potential; **EE:** Entrapment Efficiency; **CQAs:** Critical Quality Attributes; **CPPs:** Critical Process Parameters; **QbD:** Quality by Design; **PBS:** Phosphate Buffer Saline; **DCP:** Dicetyl Phosphate; **HPMC:** Hydroxypropyl Methylcellulose; **Na-CMC:** Sodium Carboxymethyl Cellulose; **PG:** Propylene Glycol; **EVA:** Ethylene Vinyl Acetate; **PVP:** Polyvinylpyrrolidone; **UV:** Ultraviolet.

SUMMARY

The study aimed to develop and optimize loratadine-loaded niosomal transdermal patches to improve drug delivery and provide a viable alternative to oral allergy treatments. Using a Box-Behnken Design (BBD) in Design Expert software, researchers assessed the impact of different surfactants (Span 40 and Span 80) on vesicle characteristics such as size, zeta potential and drug entrapment efficiency. The optimized niosomal formulation (LN-14) with Span 20, Span 40 and Span 80 exhibited a vesicle size of 195±0.55 nm, a high zeta potential of -54.25±0.08 mV and an entrapment efficiency of 91.14±2.95%. This formulation was used to create transdermal patches via solvent casting. The patches demonstrated consistent thickness, weight, flexibility and strong tensile properties. The loratadine-loaded niosomal patches showed a sustained release profile with over 40% drug permeation by the 4th hr and continued release over 42 hr. This suggests that niosomal patches could effectively deliver loratadine transdermally, offering a promising alternative to oral administration and potentially minimizing gastrointestinal side effects.

REFERENCES

1. Wong WF, Ang KP, Sethi G, Looi CY. Recent advancement of medical patch for transdermal drug delivery. Medicina. 2023;59(4):778.
2. Yilmaz EG, Ece E, Erdem Ö, Eş I, Inci F. A sustainable solution to skin diseases: ecofriendly transdermal patches. Pharmaceutics. 2023;15(2):579.
3. Tyeb S, Verma V, Kumar N. Polysaccharide based transdermal patches for chronic wound healing: Recent advances and clinical perspective. Carbohydrate Polymers. 2023;316:121038.
4. Yi S, Xie J, Chen L, Xu F. Preparation of loratadine orally disintegrating tablets by semi-solid extrusion 3D printing. Current Drug Delivery. 2023;20(6):818-29.
5. Van Nguyen K, Dang TK, Vu LTD, Ha NT, Truong HD, Tran TH. Orodispersible film incorporating nanoparticulate loratadine for an enhanced oral bioavailability. Journal of Pharmaceutical Investigation. 2023;53(3):417-26.
6. Fouziya B, Hindustan AA, Dontha SC, Jagarlamudi SV, Reddy UC, Reddy PN. Fabrication and evaluation of cefpodoxime proxetil niosomes. Asian Journal of Pharmacy and Technology. 2022;12(2):109-12.
7. Izhar MP, Hafeez A, Kushwaha P, Simrah. Drug delivery through niosomes: a comprehensive review with therapeutic applications. Journal of Cluster Science. 2023;34(5):2257-73.
8. Ghazwani M, Hani U, Alam A, Alqarni MH. Quality-by-design-assisted optimization of carvacrol oil-loaded niosomal gel for anti-inflammatory efficacy by topical route. Gels. 2023;9(5):401.
9. Lin Y-K, Hsiao C-Y, Alshetaili A, Aljuffali IA, Chen E-L, Fang J-Y. Lipid-based nanoformulation optimization for achieving cutaneous targeting: Niosomes as the potential candidates to fulfill this aim. European journal of pharmaceutical sciences. 2023;186:106458.
10. Ghumman SA, Ijaz A, Noreen S, Aslam A, Kausar R, Irfan A, *et al.* Formulation and characterization of curcumin niosomes: Antioxidant and cytotoxicity studies. Pharmaceuticals. 2023;16(10):1406.
11. Kattar A, Quelle-Regaldie A, Sánchez L, Concheiro A, Alvarez-Lorenzo C. Formulation and characterization of epalrestat-loaded polysorbate 60 cationic niosomes for ocular delivery. Pharmaceutics. 2023;15(4):1247.
12. Pires PC, Paiva-Santos AC, Veiga F. Liposome-derived nanosystems for the treatment of behavioral and neurodegenerative diseases: the promise of niosomes, transfersomes and ethosomes for increased brain drug bioavailability. Pharmaceuticals. 2023;16(10):1424.
13. Reddy PL, Shanmugasundaram S. Optimizing Process Parameters for Controlled Drug Delivery: A Quality by Design (QbD) Approach in Naltrexone Microspheres. AAPS PharmSciTech. 2024;25(5):105.
14. Kumar LS, Ahad HA. Quality by design based quercetin hydrate nanoemulsions for enhanced solubility by reducing particle size. Ind J Pharm Edu Res. 2023;57(3):965-70.
15. Chinthaginjala H, Ahad HA, Srinivasa SK, Yaparla SR, Buddadasari S, Hassan JA, *et al.* Central Composite Design Assisted Formulation Development and Optimization of Gastroretentive Floating Tablets of Dextromethorphan Hydrobromide. Ind J Pharm Edu Res. 2023;57(4):983-92.
16. Chinthaginjala H, Ahad HA, Bhargav E, Pradeepkumar B. Central composite design aided formulation development and optimization of Clarythromycin extended-release tablets. Indian Journal of Pharmaceutical Education and Research. 2021;55(2):395-406.
17. Rezaei H, Iranbakhsh A, Sepahi AA, Mirzaie A, Larijani K. Formulation, preparation of niosome loaded zinc oxide nanoparticles and biological activities. Scientific Reports. 2024;14(1):16692.
18. Soni S, Baghel K, Soni ML, Kashaw SK, Soni V. Size-dependent effects of niosomes on the penetration of methotrexate in skin layers. Future Journal of Pharmaceutical Sciences. 2024;10(1):48.
19. Akbari J, Saeedi M, Morteza-Semnani K, Sanaee A, Lotfi A, Rahimnia SM, *et al.* Green preparation, charetrization, *in vitro/in vivo* safety assessment and *in vivo* pain management of nortriptyline HCl loaded in niosome (norosome) manufactured by ecofriendly green method. Journal of Dispersion Science and Technology. 2024;45(4):819-31.
20. Harini K, Alomar SY, Vajagathali M, Manoharadas S, Thirumalai A, Girigoswami K, *et al.* Niosomal Bupropion: Exploring Therapeutic Frontiers through Behavioral Profiling. Pharmaceuticals. 2024;17(3):366.
21. Sharifi-Azad M, Zenjanab MK, Shahpouri M, Adili-Aghdam MA, Fathi M, Jahanban-Esfahlan R. Codelivery of methotrexate and silibinin by niosome nanoparticles for enhanced chemotherapy of CT26 colon cancer cells. Biomedical Materials. 2024;19(5):055015.
22. Shravani Y, Ahad HA, Haranath C, gari Poojitha B, Rahamathulla S, Rupasree A. Past Decade Work Done On Cubosomes Using Factorial Design: A Fast Track Information for Researchers. Int J Life Sci Pharma Res.(2021)11(1):P124-35.
23. Babu GN, Muthukaruppan M, Ahad HA. Impact of *Azadirachta indica* Fruit Mucilage on particle size and swelling index in Central Composite Designed Acyclovir mucoadhesive microspheres. Baghdad Science Journal. 2023;20(2):0425-.
24. Ahad HA, Kumar GA, Chinthaginjala H, Gnaneswar P, Baba HA, Krishna A. A Quick Reference to the Decade's Literature Reviewed on Ocular Films. Journal of Young Pharmacists. 2022;15(1):49-54.
25. Harsha SS, Ahad HA, Haranath C, Dasari RR, Gowthami M, Varam NJ, *et al.* Exfoliation technique of composing and depictions of clopidogrel bisulphate afloat microspheres. Journal of Evolution of Medical and Dental Sciences. 2020;9(14):1156-61.
26. Mowlaeifar MH, Niakousari M, Hosseini SMH, Eskandari MH. Effect of cholesterol to vitamin D3 and Span 60 to Tween 60 ratios on the characteristics of niosomes: variable optimization using response surface methodology (RSM). Journal of Food Quality. 2022;2022(1):7005531.
27. Moghddam SRM, Ahad A, Aqil M, Imam SS, Sultana Y. Formulation and optimization of niosomes for topical diacerein delivery using 3-factor, 3-level Box-Behnken design for the management of psoriasis. Materials science and engineering: C. 2016;69:789-97.
28. Tariq F, Zaman M, Waqar MA, Saeed MA, Sarfraz RM. Design, optimization and characterization of niosomal and polymeric nanoparticles. International Journal of Polymeric Materials and Polymeric Biomaterials. 2024;73(15):1353-66.
29. Akbarzadeh I, Shayan M, Bourbour M, Moghtaderi M, Noorbazargan H, Eshrati Yeganeh F, *et al.* Preparation, optimization and in-vitro evaluation of curcumin-loaded niosome@ calcium alginate nanocarrier as a new approach for breast cancer treatment. Biology. 2021;10(3):173.

30. Ahad HA, Kumar BP, Haranath C, Reddy KS. Fabrication and evaluation of glimepiride Ficus benghalensis fruit mucilage matrix transdermal patches. International Journal of Chemical Sciences. 2009;7(4):2294-8.
31. Ahad HA, Chinthaginjala H, Priyanka MS, Raghav DR, Gowthami M, Jyothi VN. Datura stramonium Leaves Mucilage Aided Buccoadhesive Films of Aceclofenac using 3^2 Factorial Design with Design-Expert Software. Indian Journal of Pharmaceutical Education and Research. 2021;55.
32. Islam R, Nabila FH, Wakabayashi R, Kamiya N, Moniruzzaman M, Goto M. Ionic Liquid-Based patch formulation for enhanced transdermal delivery of sparingly soluble drug. Journal of Molecular Liquids. 2024;397:124184.
33. Zheng L, Chen Y, Gu X, Li Y, Zhao H, Shao W, *et al.* Co-delivery of drugs by adhesive transdermal patches equipped with dissolving microneedles for the treatment of rheumatoid arthritis. Journal of Controlled Release. 2024;365:274-85.
34. Ashfaq A, Riaz T, Waqar MA, Zaman M, Majeed I. A comprehensive review on transdermal patches as an efficient approach for the delivery of drug. Polymer-Plastics Technology and Materials. 2024;63(8):1045-69.
35. Thakur N, Goswami M, Deka Dey A, Kaur B, Sharma C, Kumar A. Fabrication and Synthesis of Thiococlchicoside Loaded Matrix Type Transdermal Patch. Pharmaceutical Nanotechnology. 2024;12(2):143-54.
36. Abdul Razzaq A, Riaz T, Zaman M, Waqar MA, Ashfaq A. Recent advancements and various potential applications of transdermal patches. International Journal of Polymeric Materials and Polymeric Biomaterials. 2024:1-12.
37. Alwossabi AM, Albegali AA, Al-Ghani AM, Albaser NA, Alnamer RA. Advancements in Transdermal Drug Delivery Systems: Innovations, Applications and Future Directions. Al-Razi University Journal for Medical Sciences. 2024;8(2).
38. Bhattacharyya S, Mohan U. Formulation and *In vitro* Evaluation of Niosomal Gel of Loratadine: A Novel Topical Agent for Allergic Skin. Indian J Pharm Sci. 2023;85(2):325-37.
39. Sailaja C, Bhupalam PK. A Box Behnken Design Optimized Nano Vesicular Transdermal Patch for Allergies. International Journal of Pharmaceutical Investigation. 2024;14(1).
40. Teaima MH, El Mohamady AM, El-Nabarawi MA, Mohamed AI. Formulation and evaluation of niosomal vesicles containing ondansetron HCL for trans-mucosal nasal drug delivery. Drug development and industrial pharmacy. 2020;46(5):751-61.
41. Shah P, Goodyear B, Haq A, Puri V, Michniak-Kohn B. Evaluations of quality by design (QbD) elements impact for developing niosomes as a promising topical drug delivery platform. Pharmaceutics. 2020;12(3):246.
42. Kamani P, Parikh K, Kapadia R, Sawant K. Phospholipid based ultra-deformable nanovesicular gel for transcutaneous application: QbD based optimization, characterization and pharmacodynamic profiling. Journal of Drug Delivery Science and Technology. 2019;51:152-63.
43. Alnaim AS, Shah H, Nair AB, Mewada V, Patel S, Jacob S, *et al.* Qbd-based approach to optimize niosomal gel of levosulpiride for transdermal drug delivery. Gels. 2023;9(3):213.
44. Mirzaie A, Peirovi N, Akbarzadeh I, Moghtaderi M, Heidari F, Yeganeh FE, *et al.* Preparation and optimization of ciprofloxacin encapsulated niosomes: A new approach for enhanced antibacterial activity, biofilm inhibition and reduced antibiotic resistance in ciprofloxacin-resistant methicillin-resistance *Staphylococcus aureus*. Bioorganic chemistry. 2020;103:104231.
45. Heidari F, Akbarzadeh I, Nourouzian D, Mirzaie A, Bakhshandeh H. Optimization and characterization of tannic acid loaded niosomes for enhanced antibacterial and anti-biofilm activities. Advanced Powder Technology. 2020;31(12):4768-81.
46. Shah HS, Gotecha A, Jetha D, Rajput A, Bariya A, Panchal S, *et al.* Gamma oryzanol niosomal gel for skin cancer: formulation and optimization using quality by design (QbD) approach. AAPS Open. 2021;7:1-15.
47. Shahiwala AF, Qawoogha SS, Faruqui N. Designing optimum drug delivery systems using machine learning approaches: A prototype study of niosomes. AAPS PharmSciTech. 2023;24(4):94.
48. Zaid Alkilani A, Musleh B, Hamed R, Swellmeen L, Basheer HA. Preparation and characterization of patch loaded with clarithromycin nanovesicles for transdermal drug delivery. Journal of Functional Biomaterials. 2023;14(2):57.

Cite this article: Sailaja C, Bhupalam PK. Optimizing Loratadine Delivery: Development of Niosomal Transdermal Patches. Indian J of Pharmaceutical Education and Research. 2025;59(2s):s443-s453.